

# Exploring T-carbon for Energy Applications

Guangzhao Qin,<sup>1</sup> Kuan-Rong Hao,<sup>2</sup> Qing-Bo Yan,<sup>3, a)</sup> Ming Hu,<sup>1, b)</sup> and Gang Su<sup>2,4, c)</sup>

<sup>1)</sup>*Department of Mechanical Engineering, University of South Carolina, Columbia, SC 29208, USA*

<sup>2)</sup>*School of Physical Sciences, University of Chinese Academy of Sciences, Beijing 100049, China*

<sup>3)</sup>*College of Materials Science and Opto-Electronic Technology, University of Chinese Academy of Sciences, Beijing 100049, China*

<sup>4)</sup>*Kavli Institute for Theoretical Sciences, and CAS Center for Excellence in Topological Quantum Computation, University of Chinese Academy of Sciences, Beijing 100190, China*

(Dated: 2 April 2019)

Seeking for next-generation energy sources that are economic, sustainable (renewable), clean (environment-friendly), and abundant in earth is crucial when facing the challenges of energy crisis. There have been numerous studies exploring the possibility of carbon based materials to be utilized in future energy applications. In this paper, we introduce T-carbon, which is a theoretically predicted but recently experimentally synthesized carbon allotrope, as a promising material for next-generation energy applications. It is shown that T-carbon can be potentially used in thermoelectrics, hydrogen storage, lithium ion batteries, *etc.* The challenges, opportunities, and possible directions for future studies of energy applications of T-carbon are also addressed. With the development of more environment-friendly technologies, the promising applications of T-carbon in energy fields would not only produce scientifically significant impact in related fields but also lead to a number of industrial and technical applications.

## I. INTRODUCTION

With the rapid development of human society and global economy, the expense of resources has increased progressively, especially since the first industrial revolution<sup>1</sup>. The existing fossil fuels in earth such as coal, oil and natural gas, which were accumulated in the past billions of years, would be probably exhausted in hundreds years due to the huge energy demand. The approaching to resource exhaustion and the accompanying production of environmentally harmful by-products push us to find possible solutions for future energy. This could be remedied in two ways. One is to promote current utilization efficiency of energy, and to develop novel technologies to reduce the waste of energy, and to collect waste heat for reuse. The other is to find sustainable energy, renewable sources, clean fuels, *etc.*

It is known that large amount of energy is wasted in factories, home cooking and vehicle driving because of the low efficiency of energy conversion. To name a few, the efficiency of engine is about 25-50%, where the remaining part of energy is dispersed to nature in the form of waste heat, which makes serious environmental pollution and the waste of a lot of resources. If the waste heat can be recycled, we would improve fundamentally the efficiency of energy utilization and solve, to some extent, the current energy and environmental problems. On the other hand, carbon dioxide and monoxide as well as dust particles such as PM 2.5 are harmful by-products

when consuming fossil fuels, which are responsible for the global warming due to greenhouse effect and are very harmful to individual's health in addition to the environmental pollution. Thus, it is on demands to solve these challenges by seeking for next-generation energy sources that should be economic, sustainable (renewable), clean (environment-friendly), and abundant in earth.

There have been numerous studies exploring the possible utilization of carbon based materials for next-generation energy applications due to the promising physical and chemical properties<sup>2-5</sup>. However, large-scale fabrication of carbon materials or carbon based nanostructures is a formidable challenge<sup>6</sup>. Lots of efforts have been dedicated to the synthesis processes, such as the bottom-up approaches from designed carbon molecules,<sup>7</sup> the pseudo-topotactic conversion of carbon nanotubes by picosecond pulsed-laser irradiation,<sup>8</sup> *etc.* Benefited from the progress and emergence of new synthetic technology, the synthesis of novel carbon materials becomes feasible. Recently, T-carbon, which is a previously predicted carbon allotrope by theoretical study,<sup>9</sup> was experimentally synthesized (Figure 2G,H)<sup>8</sup>.

Herein, we would like to introduce T-carbon and discuss its promising applications for next-generation energy technologies (Figure 1 and Figure 2). It is shown that T-carbon can be potentially used in thermoelectrics, hydrogen storage, lithium ion batteries (Figure 3), *etc.* The challenges, opportunities, and possible directions for future studies of energy applications of T-carbon are also addressed.

<sup>a)</sup>Electronic mail: yan@ucas.ac.cn

<sup>b)</sup>Electronic mail: hu@sc.edu

<sup>c)</sup>Electronic mail: gsu@ucas.ac.cn

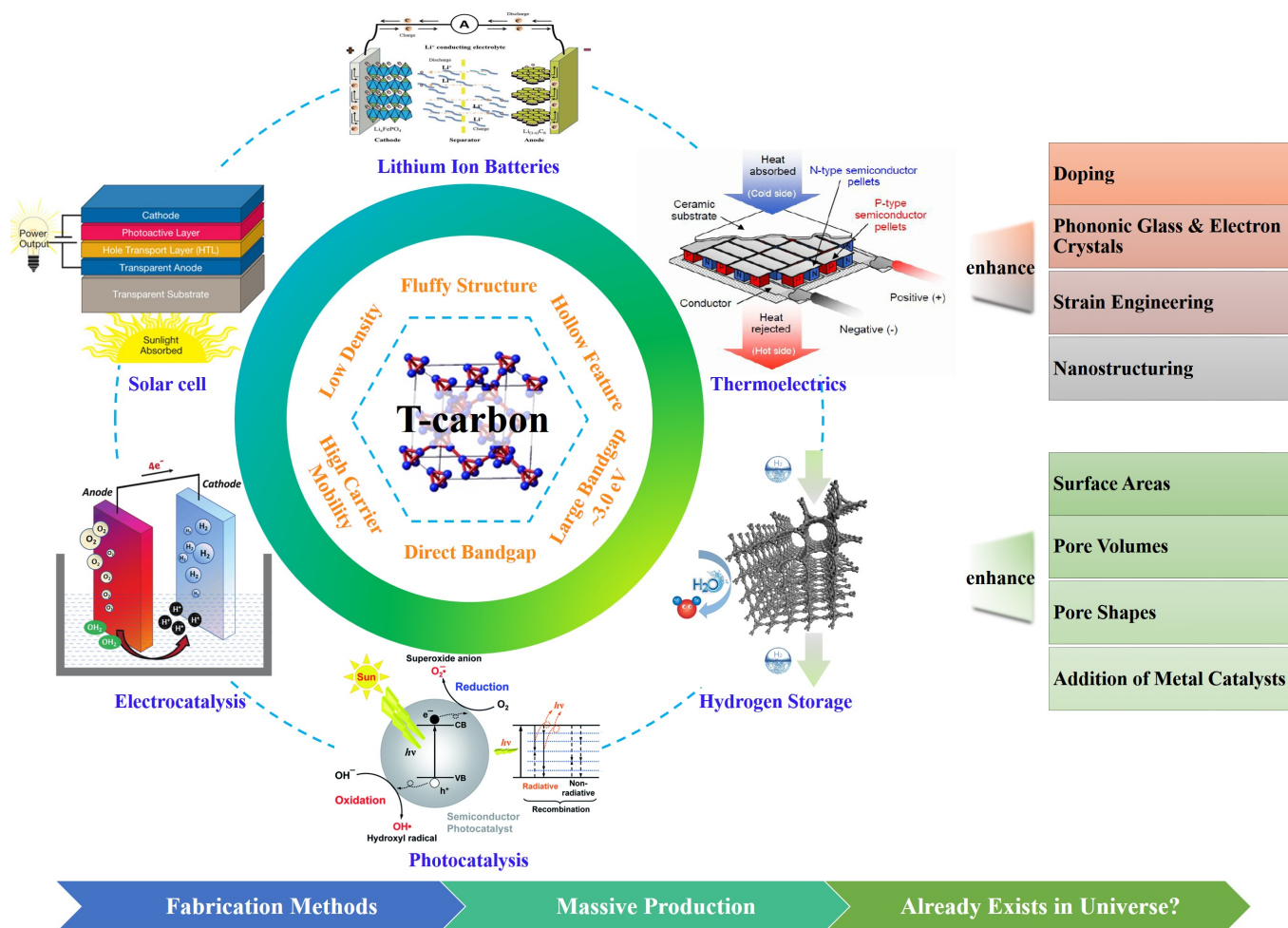


FIG. 1. Overview for T-carbon of properties, energy applications, possible enhancement approaches for thermoelectrics and hydrogen storage, and future development. Reproduced with permission.<sup>10–12</sup> Copyright 2014, 2016, Royal Society of Chemistry. Reproduction with permission available at <https://www.sigmaaldrich.com/technical-documents/articles/technology-spotlights/plexcore-pv-ink-system.html>, <http://toroccoscoolingandheating.com/thermoelectric-wine-coolers-work/>

## II. T-CARBON

Carbon is one of the most abundant elements on earth and one of the most important elements for life, which is contained in majority of molecules. Carbon atoms possess unique ability to form bonds with other carbon atoms and nonmetallic elements in diverse hybridization states ( $sp$ ,  $sp^2$ ,  $sp^3$ )<sup>4,13</sup>. Countless carbon-based organic compounds in the form of a wide range of structures from small molecules to long chains are generated, which have great diversity in the chemical and biological properties and thus result in the present colorful world<sup>2</sup>. Carbon mainly exists as three natural allotropes, namely graphite, diamond, and amorphous carbon (Figure 2A,B,C)<sup>14</sup>. Despite the same and exclusive component of carbon atoms, their properties are drastically different from each other, which is a strong hint of the diversity in the properties of carbon materials with different structures and orbital hybridizations. Over the last

several decades, several new carbon allotropes have been synthesized with novel properties and potential applications in technology. The three most typical examples include zero-dimensional (0D) fullerenes discovered in 1985 (Figure 2D), one-dimensional (1D) carbon nanotubes identified in 1991 (Figure 2E), and two-dimensional (2D) graphene isolation in 2004 (Figure 2F)<sup>15</sup>. The fantastic properties of these carbon allotropes and their highly expected engineering probabilities have attracted intensive attention from both academia and industry<sup>5</sup>.

Beyond that, a number of three-dimensional (3D) carbon allotropes have also been predicted theoretically, including M-carbon,<sup>16</sup> bct-C<sub>4</sub>,<sup>17</sup> BCO-C<sub>16</sub>,<sup>18</sup> etc, where T-carbon predicted in 2011<sup>9</sup> is the most impactful form (Figure 2G). T-carbon can be simply derived by substituting each carbon atom in cubic diamond with a C<sub>4</sub> unit of carbon tetrahedron (Figure 2C,G), and it is where the name of ‘T-carbon’ comes from. The space group of T-carbon is  $Fd\bar{3}m$ , the same as cubic diamond. There exist two tetrahedrons (eight carbon atoms in total) in a

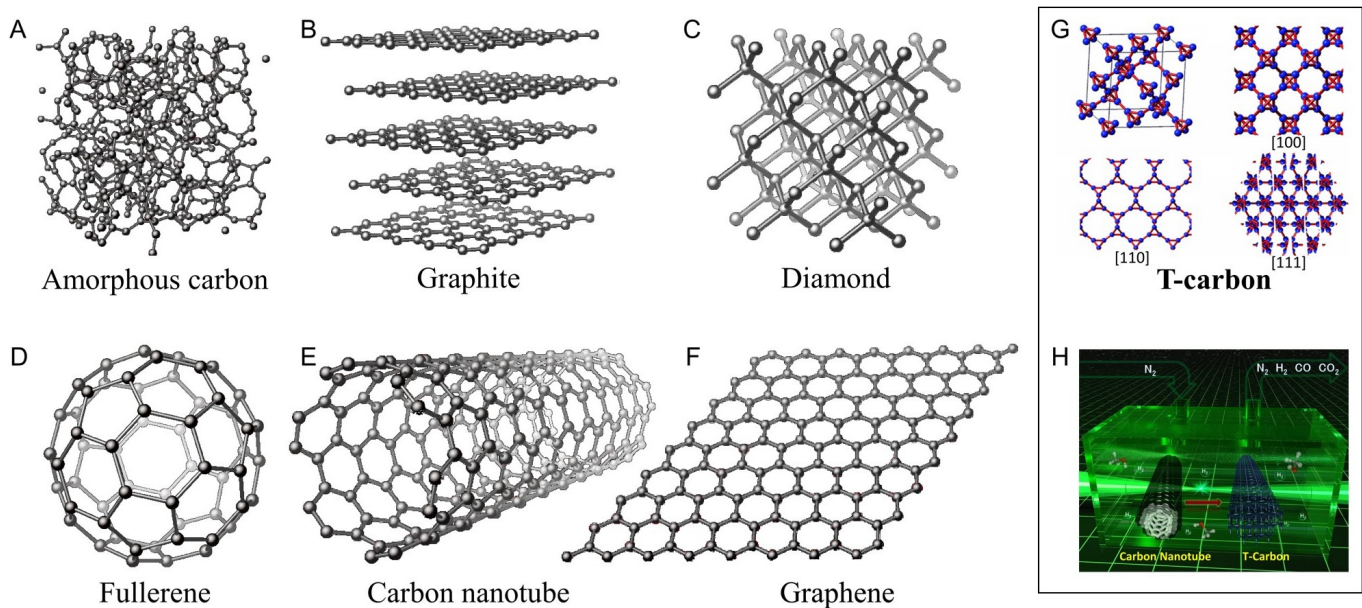


FIG. 2. The position of T-carbon in the carbon family as compared with the common carbon materials in (A-C) three-dimensional (amorphous carbon, graphite, diamond), (F) two-dimensional (graphene), (E) one-dimensional (carbon nanotube), and (D) zero-dimensional (fullerene). (G) The crystal structure of T-carbon (its space group  $Fd\bar{3}m$  is the same as cubic diamond) is generated by replacing each atom in cubic diamond with a carbon tetrahedron ( $C_4$  unit). The numbers in [] indicate the crystal direction. (H) The experimental synthesis layout of T-carbon from a pseudo-topotactic conversion of multi-walled carbon nanotubes under picosecond pulsed-laser irradiation in methanol. Reproduced with permission.<sup>9</sup> Copyright 2011, American Physical Society. Reproduction with permission available at <http://gr.xjtu.edu.cn/web/jinying-zhang/publications>.

unit cell. Such geometric configuration of carbon atoms that forms 3D T-carbon is thermodynamically stable, which is confirmed by the non-imaginary frequency of the phonon dispersion in previous study<sup>9</sup>. The lattice constant of the fully optimized T-carbon is about 7.52 Å, which is more than two times that of diamond (3.566 Å). As compared to the bond length in diamond (1.544 Å), the bonds in T-carbon possess two types with the bond length being 1.502 and 1.417 Å for intratetrahedron and intertetrahedron, respectively<sup>19</sup>. Besides, different from the bond angle in diamond ( $109.5^\circ$ ), the bond angle in T-carbon are 60 and  $144.74^\circ$  for the bonds in tetrahedron and two inequivalent bonds, respectively, implying the existence of strain. Because of the large interspaces between atoms in T-carbon, the density is  $1.50 \text{ g/cm}^3$ , which is much smaller compared to that of diamond, graphite, M-carbon, and bct- $C_4$ <sup>9</sup>. In addition to the low density, the Vickers hardness of T-carbon is calculated to be 61.1 GPa, which is around 1/3 softer than diamond (96 GPa)<sup>9,20</sup>. The low density with large interspaces between atoms and the soft nature would promise broad applications of T-carbon.

T-carbon has recently been synthesized in experiment (Figure 2H) from a pseudo-topotactic conversion of multi-walled carbon nanotube (MWCNTs) suspended in methanol under picosecond pulsed-laser irradiation<sup>8</sup>. Firstly, MWCNTs (length:  $\sim 100\text{-}200 \text{ nm}$ ; diameter:  $\sim 10\text{-}20 \text{ nm}$ ) are prepared by chemical vapor deposition (CVD) and subsequent processing. After dispersed in

absolute methanol, the suspension containing individualized MWCNTs are then transferred to the self-designed process with laser irradiation, which is stirred with a magnetic stirring bar and kept under the nitrogen atmosphere. In the fast and far-from-equilibrium process, the metastable structure is captured with the successfully transition from  $sp^2$  to  $sp^3$  chemical bonds (Figure 2H) and the suspension becomes transparent after the laser reaction. Hollow carbon nanotubes are transformed into solid carbon nanorods, where the connections between carbon atoms are exactly the same as the theoretical predicted T-carbon, demonstrating the synthesis of this kind of structure. During the transformation process, the time scale of energy transfer from the laser to the MWCNTs and the subsequent ultrafast quenching play a key role in the formation and stabilization of T-carbon. The cubic crystal system of the generated T-carbon NWs is confirmed by the fast Fourier transform (FFT) pattern at different tilting angles from the high-resolution transmission electron microscopy (HRTEM) image. The successful synthesis of T-carbon makes it joining in the carbon family as another achievable 3D carbon allotrope in addition to graphite, diamond, and amorphous carbon (Figure 2).

T-carbon's proposal and then experimental realization is a breakthrough in carbon science<sup>21,22</sup>. Compared with other allotropes of carbon, T-carbon has many unique and intriguing properties (Figure 1), suggesting that it could have a wide variety of potential applications in

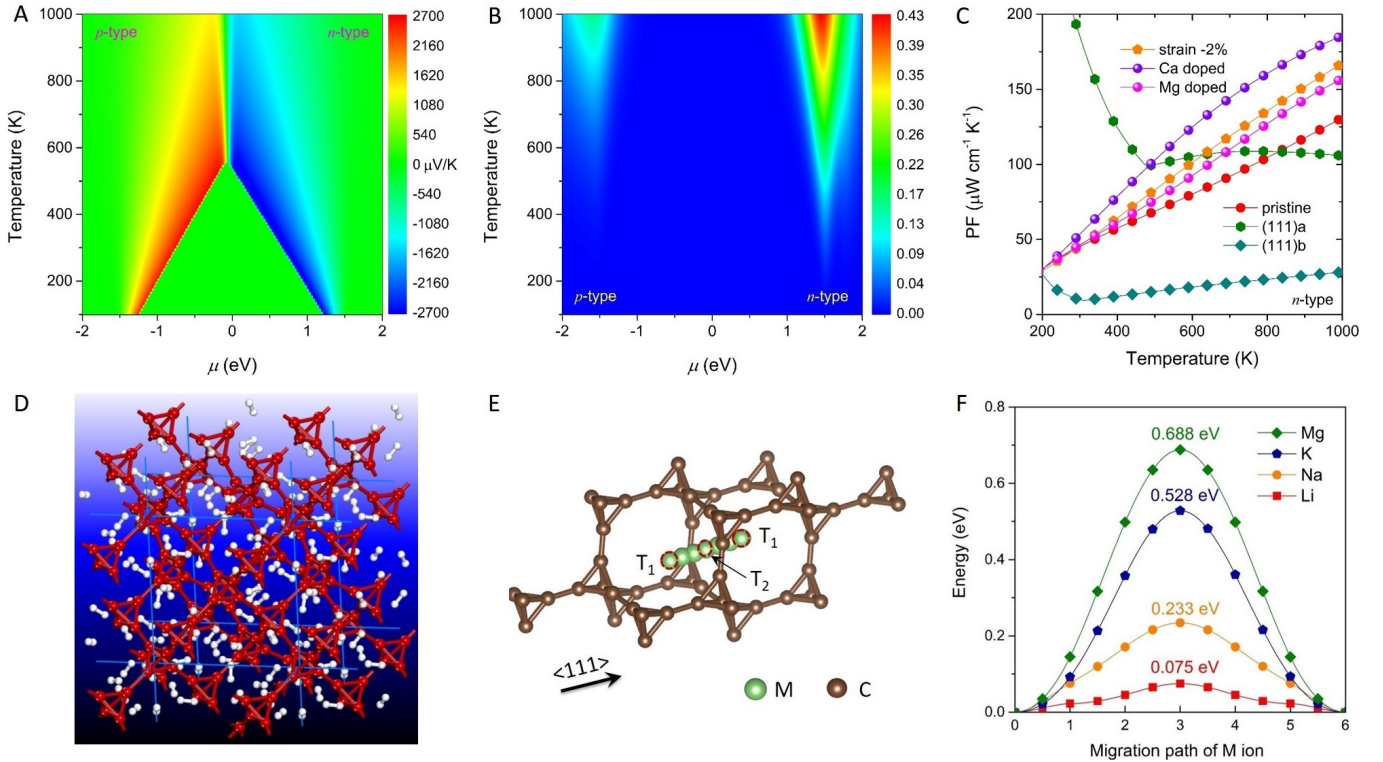


FIG. 3. The typical energy applications of T-carbon in (A-C) thermoelectrics, (D) hydrogen storage, and (E,F) lithium ion batteries (LIB). (A) Seebeck coefficient (thermopower) and (B) the figure of merit  $ZT$  in contour plot in plane of chemical potential ( $\mu$ ) and temperature. (C) The modulation of the power factor (PF) of T-carbon with compressive strain of 2% applied, with calcium (Ca) or magnesium (Mg) doped, or being cut into two-dimensional structures along the (111) direction. (D) The hydrogen storage in T-carbon with the capacity of  $\sim 7.7$  wt%. (E) The overview of M (= Li/Na/K/Mg) atoms migration in T-carbon. The minimum migration path is between  $T_1$  and the neighboring  $T_1$  sites, which are the center of the vacancy.  $T_2$  indicates the middle point. (F) The energy profiles of Li, Na, K and Mg atoms diffusing along the minimum migration path as indicated in (E).

photocatalysis, solar cells, adsorption, energy storage, supercapacitors, aerospace materials, electronic devices, *etc.* For example, T-carbon is predicted to be a semiconductor with direct band gap of  $\sim 3.0$  eV at  $\Gamma$ -point (GGA: 2.25 eV; HSE06: 2.273 eV; B3LYP: 2.968 eV)<sup>9,23</sup>. The orbitals in T-carbon hybridize with each other and form anisotropic  $sp^3$  hybridized bonds. As for the two types of bonds in T-carbon, the charge density is found to be much larger for the intertetrahedron bonds compared to the intratetrahedron bonds, indicating relatively stronger intertetrahedron bond strength with more accumulated electrons. The bond strength is consistent with the bond length, which stabilize the structure by balancing the strain from the carbon tetrahedron cage. Moreover, the band gap could be effectively adjusted by doping elements or strain engineering to be suitable for photocatalysis and solar cells<sup>23–25</sup>. Particularly, the band gap can be tuned in the range of 1.62–3.63 eV with group IVA single-atom substitution, where the doped structures hold the stability<sup>25</sup>. Quite recently, it was shown that T-carbon nanowire exhibits better ductility and larger failure strain than other carbon materials such as diamond and diamond-like carbon<sup>26</sup>. It was also reported

that the transport properties of T-carbon can be effectively modulated by imposing strain<sup>23</sup>. With the specific characteristics of the electronic band structures such as the potential efficient electron transport,<sup>23</sup> T-carbon has the potential to be used as thermoelectric materials for energy recovery and conversion,<sup>27</sup> especially after doping or strain engineering. Besides, owing to its ‘fluffy’ crystal structure, T-carbon is also possible for the storage of hydrogen, lithium, and other small molecules for energy purposes. In the following, the specific applications of T-carbon in thermoelectrics, hydrogen storage, and lithium ion batteries will be discussed in details to illustrate its potential applications in future energy fields.

### III. THERMOELECTRICS

In the sense of ‘turning waste into treasure’, the thermoelectric power generation has received extensive attention in recent years due to the low cost of operation. By achieving the output voltage through temperature gradient based on the Seebeck effect, the thermoelectrics shows a strong capability of firsthand solid-state con-

version to electrical power from thermal energy, especially from the reuse of waste heat<sup>28</sup>, thereby revealing its valued applications in reusing resources and being helpful for the crisis of environment and the save of energy. Generally, the thermoelectric efficiency and performance can be characterized by a dimensionless figure of merit  $ZT = S^2\sigma T/\kappa$ ,<sup>29</sup> where  $S$ ,  $\sigma$ ,  $T$  and  $\kappa$  represent the thermopower (Seebeck coefficient), electrical conductivity, absolute temperature and total thermal conductivity, respectively. To approach the Carnot coefficient, a high energy generation efficiency is necessary, which corresponds to a large  $ZT$ . The continuous improvement of thermoelectric performance and the strive to increase the power output under the same heat source are the key focus in the thermoelectric technology, which demands the in-depth study of thermoelectric conversion materials and the development of new materials.

Based on electronic structures and previously studied thermal transport properties of T-carbon<sup>27</sup>, we examined the thermoelectric performance of T-carbon by combining the first-principles calculations with the semi-classical Boltzmann transport theory<sup>29,30</sup>. The thermopower of T-carbon shown in Figure 3A ( $\sim 2000 \mu\text{V}/\text{K}$ ) is comparable with or even larger than some excellent thermoelectric materials, such as SnSe ( $\sim 550 \mu\text{V}/\text{K}$ )<sup>31</sup> that was reported to have an unprecedented high  $ZT$  value. The huge thermopower of T-carbon indicates its strong potential capable of serving as a thermoelectric material for energy recovery and conversion.

The overall view of evaluated  $ZT$  value of T-carbon shows that it is a high-temperature  $n$ -type thermoelectric material (Figure 3B). However, the thermoelectric performance of T-carbon is not good enough compared with other existing thermoelectric materials<sup>28</sup>. For instance, SnSe possesses a  $ZT$  value of 2.6 at 930 K along a specific lattice direction<sup>31</sup>. The reasons could lie in two aspects. Firstly, the electronic energy band gap of T-carbon is relatively large, and the conduction band minimum (CBM) and valence band maximum (VBM) are relatively flat, which may lead to a large effective mass of the carriers and lower the electrical conductivity. Secondly, the thermal conductivity of T-carbon at room temperature is  $33 \text{ W}/\text{mK}$ ,<sup>27</sup> which is much higher for thermoelectric applications in contrast to that of SnSe ( $0.46\text{-}0.68 \text{ W}/\text{mK}$ )<sup>31</sup>.

Nevertheless, there exists a large room for further improving the thermoelectric performance of T-carbon in view of its excellent thermopower through, *e.g.* applying strain,<sup>29</sup> doping proper elements,<sup>32</sup> or cutting into low-dimensional structures to modify transport properties<sup>33</sup>. We then examined possible approaches for the improvement of the thermoelectric performance of T-carbon. As shown in Figure 3C, by either applying compressive strain of 2% or doping calcium (Ca) and magnesium (Mg) atoms into the fluffy structure of T-carbon, the power factor can be effectively improved. We focus on the  $n$ -type doping, since T-carbon is a  $n$ -type thermoelectric material as discussed above. The reason for the doping

enhanced power factor lies in two aspects. On the one hand, with Ca/Mg atoms doped, the characteristics of conduction band is kept, promising a large thermopower after doping. On the other hand, the electronic band gap transits from direct to indirect and is largely decreased, leading to a large electrical conductivity. Note that the thermal conductivity commonly decreases with foreigner atoms doped, thus the thermoelectric performance of T-carbon would be largely improved owing to the simultaneously improved electrical transport properties and reduced thermal transport properties.

Considering the huge computational costs, we could estimate the thermoelectric performance based on the estimated thermal conductivity with atoms doped. Assuming a one order of magnitude decrease of the thermal conductivity with Ca/Mg atoms doped, the  $ZT$  value of T-carbon is estimated to be largely enhanced with a two-fold increase. Moreover, by cutting T-carbon into two-dimensional structures along the (111) direction, the power factor can also be improved, especially at low temperatures (Figure 3C). The large power factor at low temperature makes T-carbon in nanoscale transit from the high-temperature thermoelectric material to a low-temperature thermoelectric material, suggesting its wider applications for energy conversion, such as the waste heat recovery under ambient conditions.

#### IV. HYDROGEN STORAGE

Seeking for sustainable, renewable, and clean fuels is on demand, in particular we are facing with the challenges of energy crisis and climate change. Since 1970s, hydrogen has been thought as one of the most promising alternatives to fossil fuels due to the cleanliness of its combustion. Water ( $\text{H}_2\text{O}$ ) is the only by-product for hydrogen combustion, which has great advantages compared with the combustion of fossil fuels producing greenhouse gas and harmful pollutants. Moreover, hydrogen is lightweight, providing a higher energy density and making the hydrogen-powered engines more efficient than the internal combustion engines. The reason hampering the popularization of hydrogen economy lies in that it is difficult to store large amounts of hydrogen safely, densely, rapidly, and then access easily. Lots of efforts have been dedicated to discovering new materials as next generation hydrogen storage materials, including the extremely porous metal-organic framework (MOF) compounds<sup>34</sup>.

Benefiting from the high surface area and lightweight of carbon materials, there have been many efforts in designing novel porous carbon materials for hydrogen storage applications<sup>3,13,35,36</sup>. Since T-carbon itself is a fluffy carbon material, there are large interspaces between atoms compared with other forms of carbon materials, which could make it potentially useful for hydrogen storage (Figure 1 and Figure 3D). In fact, T-carbon possesses a low density ( $\sim 1.50 \text{ g}/\text{cm}^3$ ) as mentioned above, which is approximate  $2/3$  of graphite and  $1/2$  of diamond<sup>9</sup>. By

absorbing hydrogen into the fluffy structure of T-carbon, the hydrogen storage value can be estimated based on the number of adsorbed hydrogen molecules ( $H_2$ ), which is 16 in maximum for one unit cell in a stable structure. The adsorption energy for hydrogen in T-carbon is defined as<sup>36</sup>

$$E_{\text{adsorption}} = [E_{\text{T-carbon}} + nE_{H_2} - E_{\text{total}}]/n, \quad (1)$$

where  $E_{\text{T-carbon}}$  is the total energy of T-carbon,  $E_{H_2}$  is the total energy of hydrogen molecules,  $n$  is the number of hydrogen molecules, and  $E_{\text{total}}$  is the total energy of T-carbon with hydrogen absorbed.  $E_{\text{adsorption}}$  is 0.173 and -0.216 eV for 8 and 16  $H_2$  absorbed, respectively. Considering the strong C-C bonding in T-carbon, the system is stable despite the weak repulsive interactions among the absorbed  $H_2$  like in fullerenes with hydrogen absorbed. With this condition, the hydrogen storage capacity of T-carbon is estimated to be  $\sim 7.7$  wt%, which makes it quite competitive for the high-capacity hydrogen storage<sup>9</sup>.

## V. LITHIUM ION BATTERIES

Rechargeable energy storage devices such as lithium ion batteries (LIB) are playing a critical role as portable power sources in electronic devices, biomedicine, aviation space and electric vehicles<sup>37</sup>. Various carbon based materials have been widely used in LIB, among which graphite is the most commonly used anode material. Due to its layered structure with high specific surface area and large interlayer space to accommodate lithium atoms, graphite has a high specific energy capacity ( $372 \text{ mAhg}^{-1}$ )<sup>38</sup>.

As a new member of carbon materials family, T-carbon could be also a promising electrode material for LIB and other rechargeable energy storage devices due to its fluffy structure. The possibilities of T-carbon acting as an electrode material for alkali metals (Li, Na, K) and alkaline earth metal (Mg) ion batteries were investigated based on first-principles calculations. The specific capacity of metal atoms is defined as  $C = nF/M_{C_X}$ ,<sup>37</sup> where  $n$  represents the number of electrons involved in the electrochemical process ( $n=1$  for Li, Na, K;  $n=2$  for Mg),  $F$  is the Faraday constant with a value of  $26.801 \text{ Ahmol}^{-1}$ ,  $M_{C_X}$  is the mass of  $C_X$  ( $C$  means carbon atoms,  $X$  means the number of carbon atoms, which is 8 for T-carbon). Our results reveal that T-carbon is a good anode material for LIB with the specific energy capacity of  $588 \text{ mAhg}^{-1}$ , which is 58% higher than that of graphite ( $372 \text{ mAhg}^{-1}$ )<sup>38</sup>. The corresponding formula is  $\text{Li}_2\text{C}_8$ , indicating that two Li ions can be intercalated in each T-carbon unit cell. The results for Na, K, and Mg are also similar, except that the specific energy capacity for Mg is  $1176 \text{ mAhg}^{-1}$  due to its doubled valence electrons.

As shown in Figure 3E, the most stable adsorption site of metallic ions was calculated to be the center of the vacancy of T-carbon, which is marked as  $T_1$  site. The migration process of M (= Li/Na/K/Mg) ions in T-carbon

was simulated by means of the climbing image nudged elastic band method (CI-NEB)<sup>39</sup> in a  $2 \times 2 \times 2$  supercell. As indicated in Figure 3E, the minimum migration path is between the neighboring  $T_1$  sites. The middle point ( $T_2$  site) corresponds to the saddle point on the potential energy surface. Figure 3F shows the energy evolution for the migration process, where the migration barriers are 0.075, 0.233, 0.528, and 0.688 eV for Li, Na, K, and Mg, respectively. The lowest barrier for ion moving from  $T_1$  to neighboring  $T_1$  sites in T-carbon is observed for Li ion.

It should be noted that the Li migration barrier in T-carbon is about 1/4 of that in graphite ( $0.327 \text{ eV}$ )<sup>38</sup>, which implies that the diffusion constant of Li ion in T-carbon should be  $1.7 \times 10^4$  times larger than that of Li ion in graphite following the Arrhenius law ( $D \sim \exp(-E/k_B T)$ , where  $E$ ,  $k_B$ , and  $T$  are barrier energy, Boltzmann constants, and temperature, respectively)<sup>40</sup>. Thus, T-carbon should be a very good material for the diffusion of Li ions, revealing that it might be quite useful for the ultrafast charge and discharge of future rechargeable energy storage devices.

## VI. OPPORTUNITIES AND CHALLENGES

Both opportunities and challenges exist for the applications of T-carbon in next-generation energy technologies (Figure 1). To achieve better thermoelectric performance of T-carbon, doping other elements can be performed by following what researchers did previously for clathrates and skutterudites,<sup>41</sup> which are hot thermoelectric materials with hollow cage-like structures. In terms of the fluffy structure with low density and hollow feature (Figure 1), the characteristics of ‘phononic glass & electron crystals’ could be realized in T-carbon by filling the holes with different kinds of atoms and different filling rates, thus reducing its thermal conductivity and simultaneously improving its electrical transport properties, which would make T-carbon a better thermoelectric material. In addition to the filling doping, one can also introduce nanotwin structures into T-carbon, which could have the similar effect<sup>42</sup>. Based on previous works, the possible interstitial atoms to improve the thermoelectric performance of T-carbon could be lanthanides, alkali metals, alkaline earth metals, and rare earth metals. Other approaches in addition to applying external fields<sup>33</sup> and bond nanodesigning,<sup>43,44</sup> such as strain engineering and nanostructuring, would also be possible (Figure 3C). Further detailed and comprehensive studies for examining possible improvement of the thermoelectric performance, especially from the experimental aspects, are expected to come in future.

In addition, with the potentially high capacity of hydrogen storage in T-carbon, the effects of different surface areas, pore volumes, and pore shapes on hydrogen storage parameters should be examined. New methods to enhance the storage capacity are necessary, such as

the addition of metal catalysts, which has been previously reported for considerably improving the capacity of hydrogen storage. With the fluffy structure, it is also possible for T-carbon to be used for storing or filtering other small molecules for energy purposes beyond the applications in LIB. Beyond the applications of T-carbon in thermoelectrics, hydrogen storage, and lithium ion batteries as discussed above, T-carbon, especially T-carbon based heterostructures,<sup>4,7,45</sup> could have a wide variety of potential applications in more energy fields (Figure 1), such as electrochemical, photocatalysis, solar cells, adsorption, energy storage, supercapacitors, aerospace, electronics, *etc.*, which are worth to be further investigated in future.

To further explore potential applications of T-carbon in energy fields, much effort on fabrication methods and massive production of T-carbon should be greatly paid (Figure 1)<sup>6</sup>. Apart from the synthesizing method reported in Ref.<sup>8</sup>, the plasma enhanced chemical vapor deposition at a proper environmental pressure is also a possible route to generate T-carbon. Particularly, T-carbon is found to be more stable and more easily formed at negative pressure circumstances since it possesses a relatively smaller enthalpy than diamond beyond negative 22.5 GPa. In addition, T-carbon could be grown from seed microparticles in a chemical vapor transport process, where the seed quality and distribution should be optimized to obtain high-quality T-carbon samples. With the development of more environment-friendly technologies, the potential applications of T-carbon in energy fields would not only produce scientifically significant impact in related fields but also lead to a number of industrial and technical applications.

Beyond the applications in energy fields, T-carbon may also contribute to solving the carbon crisis in interstellar dust<sup>46</sup>, which remains an unsolved question for decades. Observations find that the abundance of carbon in the interstellar medium is only  $\sim 60\%$  of its solar value, leading to the difficulty in explaining the interstellar extinction curve with the traditional interstellar dust models<sup>46</sup>. Due to the fluffy structure of T-carbon, its density is approximately  $2/3$  of graphite. Besides, the optical absorption of T-carbon has a sharp peak around 225 nm, which is very close to the broad ‘bump’ centered at 217.5 nm in the interstellar extinction curve<sup>8,46</sup>. Moreover, the negative pressure circumstance in the universe is beneficial for the formation of T-carbon. Thus, it would be very meaningful to explore whether T-carbon already exists in universe beyond the artificial synthesis.

## ACKNOWLEDGMENTS

G. Q. gratefully acknowledges Dr. Zhenzhen Qin (Zhengzhou University) for literature review and Dr. Huimin Wang (Nanjing University) for plotting Figure 1. G. Q. also thanks Dr. Xianlei Sheng (Beihang University) and Mr. Jingyao You (University of Chinese Academy

of Sciences) for their fruitful discussions. This work was supported in part by the National Key R&D Program of China (Grant No. 2018YFA0305800), the NSFC (Grant Nos. 11834014, 14474279), the Strategic Priority Research Program of the Chinese Academy of Sciences (Grant Nos. XDB28000000, XDPB08).

## COMPUTATION DETAILS

All calculations involved in this paper (Figure 3) were carried out by means of the first-principles calculations in the framework of density functional theory (DFT) as implemented in the Vienna *ab-initio* simulation package (VASP)<sup>47</sup>. The projector augmented wave (PAW) method<sup>48</sup> were employed for interactions between ion cores and valence electrons. The electron exchange-correlation interactions were described by the generalized gradient approximation (GGA) in the form proposed by Perdew-Burke-Ernzerhof (PBE)<sup>49</sup>. The cutoff energy was set as 1000 eV for plane-wave expansion of valence electron wave function. The structure relaxation considering both atomic positions and lattice vectors was performed until the total energy was converged to  $10^{-8}$  eV/atom and the maximum force on each atom was less than 0.001 eV/Å. The Monkhorst-Pack scheme<sup>50</sup> was used to sample the Brillouin zone (BZ) with a  $11 \times 11 \times 11$  *k*-point mesh.

<sup>1</sup>Bonaccorso, F. *et al.* Graphene, related two-dimensional crystals, and hybrid systems for energy conversion and storage. *Science* **347**, 1246501 (2015).

<sup>2</sup>Wang, L. & Hu, X. Recent advances in porous carbon materials for electrochemical energy storage. *Chemistry - An Asian Journal* **13**, 1518–1529 (2018). URL <http://doi.wiley.com/10.1002/asia.201800553>.

<sup>3</sup>Gao, Y. *et al.* Electron and phonon properties and gas storage in carbon honeycombs. *Nanoscale* **8**, 12863–12868 (2016). URL <http://xlink.rsc.org/?DOI=C6NR03655D>.

<sup>4</sup>Jayaraman, T. *et al.* Recent development on carbon based heterostructures for their applications in energy and environment: A review. *Journal of Industrial and Engineering Chemistry* **64**, 16–59 (2018). URL <https://linkinghub.elsevier.com/retrieve/pii/S1226086X18300996>.

<sup>5</sup>Tour, J. M., Kittrell, C. & Colvin, V. L. Green carbon as a bridge to renewable energy. *Nature Materials* **9**, 871 (2010). URL <http://dx.doi.org/10.1038/nmat2887>.

<sup>6</sup>Kumar, R., Joanni, E., Singh, R. K., Singh, D. P. & Moshkalev, S. A. Recent advances in the synthesis and modification of carbon-based 2d materials for application in energy conversion and storage. *Progress in Energy and Combustion Science* **67**, 115–157 (2018). URL <https://linkinghub.elsevier.com/retrieve/pii/S0360128517301612>.

<sup>7</sup>Mori, T. *et al.* Carbon nanosheets by morphology-retained carbonization of two-dimensional assembled anisotropic carbon nanorings. *Angewandte Chemie International Edition* **57**, 9679–9683 (2018). URL <http://doi.wiley.com/10.1002/anie.201803859>.

<sup>8</sup>Zhang, J. *et al.* Pseudo-topotactic conversion of carbon nanotubes to t-carbon nanowires under picosecond laser irradiation in methanol. *Nature Commun.* **8**, 683 (2017). URL <https://doi.org/10.1038/s41467-017-00817-9>.

<sup>9</sup>Sheng, X.-L., Yan, Q.-B., Ye, F., Zheng, Q.-R. & Su, G. T-carbon: A novel carbon allotrope. *Phys. Rev. Lett.* **106**, 155703

- (2011). URL <http://link.aps.org/doi/10.1103/PhysRevLett.106.155703>.
- <sup>10</sup>Lee, H., Yanilmaz, M., Toprakci, O., Fu, K. & Zhang, X. A review of recent developments in membrane separators for rechargeable lithium-ion batteries. *Energy Environ. Sci.* **7**, 3857–3886 (2014). URL <http://xlink.rsc.org/?DOI=C4EE01432D>.
- <sup>11</sup>Joya, K. S., Ahmad, Z., Joya, Y. F., Garcia-Esparza, A. T. & de Groot, H. J. M. Efficient electrochemical water oxidation in neutral and near-neutral systems with a nanoscale silver-oxide catalyst. *Nanoscale* **8**, 15033–15040 (2016). URL <http://xlink.rsc.org/?DOI=C6NR03147A>.
- <sup>12</sup>Djurić, A. B., Leung, Y. H. & Ching Ng, A. M. Strategies for improving the efficiency of semiconductor metal oxide photocatalysis. *Materials Horizons* **1**, 400 (2014). URL <http://xlink.rsc.org/?DOI=c4mh00031e>.
- <sup>13</sup>Borchardt, L. *et al.* Toward a molecular design of porous carbon materials. *Materials Today* **20**, 592–610 (2017). URL <https://linkinghub.elsevier.com/retrieve/pii/S1369702117302043>.
- <sup>14</sup>Georgakilas, V., Perman, J. A., Tucek, J. & Zboril, R. Broad family of carbon nanoallotropes: Classification, chemistry, and applications of fullerenes, carbon dots, nanotubes, graphene, nanodiamonds, and combined superstructures. *Chemical Reviews* **115**, 4744–4822 (2015). URL <http://pubs.acs.org/doi/10.1021/cr500304f>.
- <sup>15</sup>Hirsch, A. The era of carbon allotropes. *Nature Materials* **9**, 868 (2010). URL <http://dx.doi.org/10.1038/nmat2885>.
- <sup>16</sup>Li, Q. *et al.* Superhard monoclinic polymorph of carbon. *Phys. Rev. Lett.* **102**, 175506 (2009). URL <https://link.aps.org/doi/10.1103/PhysRevLett.102.175506>.
- <sup>17</sup>Umamoto, K., Wentzcovitch, R. M., Saito, S. & Miyake, T. Body-centered tetragonal  $c_4$ : A viable  $sp^3$  carbon allotrope. *Phys. Rev. Lett.* **104**, 125504 (2010). URL <https://link.aps.org/doi/10.1103/PhysRevLett.104.125504>.
- <sup>18</sup>Wang, J.-T. *et al.* Body-centered orthorhombic  $c_{16}$ : A novel topological node-line semimetal. *Phys. Rev. Lett.* **116**, 195501 (2016). URL <http://link.aps.org/doi/10.1103/PhysRevLett.116.195501>.
- <sup>19</sup>Esser, M., Esser, A. A., Proserpio, D. M. & Dronskowski, R. Bonding analyses of unconventional carbon allotropes. *Carbon* **121**, 154–162 (2017). URL <https://linkinghub.elsevier.com/retrieve/pii/S0008622317305213>.
- <sup>20</sup>Chen, X.-Q., Niu, H., Franchini, C., Li, D. & Li, Y. Hardness of t-carbon: Density functional theory calculations. *Phys. Rev. B* **84**, 121405 (2011). URL <https://link.aps.org/doi/10.1103/PhysRevB.84.121405>.
- <sup>21</sup>Xing, M., Li, B., Yu, Z. & Chen, Q. A reinvestigation of a superhard tetragonal  $sp^3$  carbon allotrope. *Materials* **9**, 484 (2016). URL <http://www.mdpi.com/1996-1944/9/6/484>.
- <sup>22</sup>Wang, J.-Q., Zhao, C.-X., Niu, C.-Y., Sun, Q. & Jia, Y. C20 t carbon: a novel superhard  $sp^3$  carbon allotrope with large cavities. *J. Phys.: Condens. Matter* **28**, 475402 (2016). URL <http://stacks.iop.org/0953-8984/28/i=47/a=475402?key=crossref.8a940650d806c49ce318eccabef29ca1>.
- <sup>23</sup>Sun, P.-P., Bai, L., Kripalani, D. R. & Zhou, K. A new carbon phase with direct bandgap and high carrier mobility as electron transport material for perovskite solar cells. *npj Computational Materials* **5**, 9 (2019). URL <http://www.nature.com/articles/s41524-018-0146-z>.
- <sup>24</sup>Alborznia, H., Naseri, M. & Fatahi, N. Pressure effects on the optical and electronic aspects of t-carbon: A first principles calculation. *Optik* **180**, 125–133 (2019). URL <https://linkinghub.elsevier.com/retrieve/pii/S0030402618318321>.
- <sup>25</sup>Ren, H., Chu, H., Li, Z., Yue, T. & Hu, Z. Efficient energy gap tuning for t-carbon via single atomic doping. *Chemical Physics* **518**, 69–73 (2019). URL <https://linkinghub.elsevier.com/retrieve/pii/S0301010418311625>.
- <sup>26</sup>Bai, L., Sun, P.-P., Liu, B., Liu, Z. & Zhou, K. Mechanical behaviors of t-carbon: A molecular dynamics study. *Carbon* **138**, 357–362 (2018). URL <https://linkinghub.elsevier.com/retrieve/pii/S0008622318306961>.
- <sup>27</sup>Yue, S.-Y. *et al.* Thermal transport in novel carbon allotropes with  $p^2$  or  $p^3$  hybridization: An ab initio study. *Phys. Rev. B* **95**, 085207 (2017). URL <https://link.aps.org/doi/10.1103/PhysRevB.95.085207>.
- <sup>28</sup>Biswas, K. *et al.* High-performance bulk thermoelectrics with all-scale hierarchical architectures. *Nature* **489**, 414 (2012). URL <http://dx.doi.org/10.1038/nature11439>.
- <sup>29</sup>Qin, G. *et al.* Hinge-like structure induced unusual properties of black phosphorus and new strategies to improve the thermoelectric performance. *Sci. Rep.* **4**, 6946 (2014).
- <sup>30</sup>Madsen, G. K. & Singh, D. J. Boltztrap, a code for calculating band-structure dependent quantities. *Comput. Phys. Commun.* **175**, 67–71 (2006). URL <http://www.sciencedirect.com/science/article/pii/S0010465006001305>.
- <sup>31</sup>Zhao, L.-D., Chang, C., Tan, G. & Kanatzidis, M. G. Snse: a remarkable new thermoelectric material. *Energy Environ. Sci.* **9**, 3044–3060 (2016). URL <http://dx.doi.org/10.1039/C6EE01755J>.
- <sup>32</sup>Gharsallah, M. *et al.* Giant seebeck effect in ge-doped SnSe. *Sci. Rep.* **6**, 26774 (2016). URL <http://www.nature.com/articles/srep26774>.
- <sup>33</sup>Qin, G. *et al.* Diverse anisotropy of phonon transport in two-dimensional group IV-VI compounds: A comparative study. *Nanoscale* **8**, 11306–11319 (2016). URL <http://dx.doi.org/10.1039/C6NR01349J>.
- <sup>34</sup>Suh, M. P., Park, H. J., Prasad, T. K. & Lim, D.-W. Hydrogen storage in metalorganic frameworks. *Chem. Rev.* **112**, 782–835 (2012). URL <https://doi.org/10.1021/cr200274s>.
- <sup>35</sup>Xu, F., Wu, D., Fu, R. & Wei, B. Design and preparation of porous carbons from conjugated polymer precursors. *Materials Today* **20**, 629–656 (2017). URL <https://linkinghub.elsevier.com/retrieve/pii/S136970211730038X>.
- <sup>36</sup>Srinivasu, K. & Ghosh, S. K. Electronic structure, optical properties, and hydrogen adsorption characteristics of supercubane-based three-dimensional porous carbon. *The Journal of Physical Chemistry C* **116**, 25015–25021 (2012). URL <http://pubs.acs.org/doi/10.1021/jp3104479>.
- <sup>37</sup>Nitta, N., Wu, F., Lee, J. T. & Yushin, G. Li-ion battery materials: present and future. *Materials Today* **18**, 252–264 (2015). URL <https://linkinghub.elsevier.com/retrieve/pii/S1369702114004118>.
- <sup>38</sup>Uthaisar, C. & Barone, V. Edge effects on the characteristics of li diffusion in graphene. *Nano Letters* **10**, 2838–2842 (2010).
- <sup>39</sup>Henkelman, G., Uberuaga, B. P. & Jonsson, H. A climbing image nudged elastic band method for finding saddle points and minimum energy paths. *J. Chem. Phys.* **113**, 9901–9904 (2000).
- <sup>40</sup>Hao, K.-R., Fang, L., Yan, Q.-B. & Su, G. Lithium adsorption and migration in group IVVI compounds and GeS/graphene heterostructures: a comparative study. *Physical Chemistry Chemical Physics* **20**, 9865–9871 (2018). URL <http://xlink.rsc.org/?DOI=C8CP00805A>.
- <sup>41</sup>Chen, G., Dresselhaus, M. S., Dresselhaus, G., Fleurial, J.-P. & Caillat, T. Recent developments in thermoelectric materials. *International Materials Reviews* **48**, 45–66 (2003). URL <http://www.tandfonline.com/doi/full/10.1179/095066003225010182>.
- <sup>42</sup>Zhou, Y., Gong, X., Xu, B. & Hu, M. Decouple electronic and phononic transport in nanotwinned structures: a new strategy for enhancing the figure-of-merit of thermoelectrics. *Nanoscale* **9**, 9987–9996 (2017). URL <http://dx.doi.org/10.1039/C7NR02557B>.
- <sup>43</sup>Qin, G., Qin, Z., Wang, H. & Hu, M. Lone-pair electrons induced anomalous enhancement of thermal transport in strained planar two-dimensional materials. *Nano Energy* **50**, 425–430 (2018). URL <http://www.sciencedirect.com/science/article/pii/S2211285518303574>.
- <sup>44</sup>Qin, G. *et al.* Resonant bonding driven giant phonon anharmonicity and low thermal conductivity of phosphorene. *Phys. Rev. B* **94**, 165445 (2016). URL <https://link.aps.org/doi/10.1103/PhysRevB.94.165445>.



- <sup>45</sup>Ram, B. & Mizuseki, H. Tetrahexcarbon: A two-dimensional allotrope of carbon. *Carbon* **137**, 266–273 (2018). URL <https://linkinghub.elsevier.com/retrieve/pii/S0008622318304937>.
- <sup>46</sup>Dwek, E. Can composite fluffy dust particles solve the interstellar carbon crisis? *The Astrophysical Journal* **484**, 779–784 (1997). URL <http://stacks.iop.org/0004-637X/484/i=2/a=779>.
- <sup>47</sup>uller, J. Efficient iterative schemes for ab initio total-energy calculations using a plane-wave basis set. *Phys. Rev. B* **54**, 11169–11186 (1996). URL <http://link.aps.org/doi/10.1103/PhysRevB.54.11169>.
- <sup>48</sup>Kresse, G. & Joubert, D. From ultrasoft pseudopotentials to the projector augmented-wave method. *Phys. Rev. B* **59**, 1758–1775 (1999). URL <http://link.aps.org/doi/10.1103/PhysRevB.59.1758>.
- <sup>49</sup>Perdew, J. P., Burke, K. & Ernzerhof, M. Generalized gradient approximation made simple. *Phys. Rev. Lett.* **77**, 3865–3868 (1996). URL <http://link.aps.org/doi/10.1103/PhysRevLett.77.3865>.
- <sup>50</sup>Monkhorst, H. J. & Pack, J. D. Special points for brillouin-zone integrations. *Phys. Rev. B* **13**, 5188–5192 (1976). URL <http://link.aps.org/doi/10.1103/PhysRevB.13.5188>.